Design and Simulation of Out-of-Plane Nanomaterial-Based Thermocouples

Aniello Falco
Paolo Lugli
Faculty of Science and Technology
Free University of Bolzano - BozenBolzano – Bozen, Italy
email: {Aniello.falco, paolo.lugli}@unibz.it

Florin-Cristian Loghin
Almudena Rivadeneyra
Institute for Nanoelectronics
Technical University of Munich
Munich, Germany
email: {florin.loghin, almudena.rivadeneyra}@tum.de

Luca Larcher
Alessandro Bertacchini
Dipartimento di Scienze e Metodi dell'Ingegneria
University of Modena and Reggio Emilia
email: {luca.larcher, Alessandro.bertacchini}@unimore.it

***Abstract*— Our contribution indicates a novel solution for the development of the field of low-cost, printed thermocouples for energy harvesting and autonomous thermal sensors. Particularly, our work stems from the observation that the totality of printed thermocouples presented in literature relies on the conversion of a thermal gradient parallel to the plane of material deposition. This strategy is inherently inefficient and rarely applicable in real life scenarios. To overcome these issues, we introduced a novel concept of printed thermocouples, which use 3D-printing to define a vertical structure, upon which an out-of-plane thermal gradient can form and be harvested. Here, we perform thermoelectrical multi-physics simulations, employing parameters of nanomaterials extracted from literature, to show how this approach can lead to generate hundreds of microwatt in typical work conditions. Given their elevated thermopower, these structures could be employed both as autonomous sensors and energy harvesters in Internet of Things applications.**

Keywords - 3D Printing; Spray-Deposition; Thermocouple; Nanomaterials; Nanotubes; Low-Cost Electronics

I. INTRODUCTION

As the concept of Internet of Things (IoT) has been steadily rising in importance and interest, the world of electronics found itself facing many complex and very exciting challenges. If, on one hand, the IoT might account for an economic impact of more than $10 trillion by 2025, on the other hand there is still a number of barriers – socio-ethical and technological - to overcome [1]. One of the main areas of needed technical progress is represented by the realization of low-cost and low-power sensors, able to provide the necessary information to the computer-centralized data-analysis structures [1][2]. Amongst the many quantities to measure and to collect, temperature is certainly one of the most important: its applications range from smart cities [3] to agriculture [4], from healthcare [5] to industrial processes [6].

However, as in autonomous or semi-autonomous IoT nodes the power supply of the sensing system is a major issue, conventional thermoresistive systems cannot be employed.

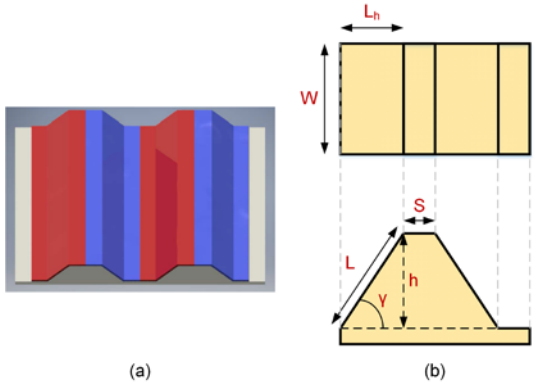

Figure 1. Concept of a 3D-Printed support for planar printed thermocouples, where the light colored material is a printable thermoplastic (e.g., ABS), the red and blue bands represent p- and n-type thermoelectric (a) The diagrams in (b) show the most important geometrical parameters

One of the strongest candidates to solve this issue is represented by printed thermoelectric devices. Differently from thermoresistors, thermocouples are able to generate a voltage across junctions of p-type and n-type thermoelectric materials. As a result, they can be employed as both differential temperature sensors and energy harvesters. Furthermore, printed thermocouples, similarly to most printed devices [7], are characterized by facile production, low-cost and arbitrary shapes [8]. Classical printed thermocouples are composed of a number of junctions between p-type and n-type thermoelectric materials, printed on a plastic (or paper) surfaces [9][10]. This system, however, presents a significant drawback: in order to function properly, they need a thermal gradient parallel to the deposition plane. Although this condition is easy to fulfill in laboratory conditions, it is far from real life applications, where typical thermal gradients are transverse to the deposition plane. Examples include, and are not limited to, heat emitted from a living body, or the temperature inside the engine of a vehicle. The solution we

 ISBN: 978-1-61208-621-7

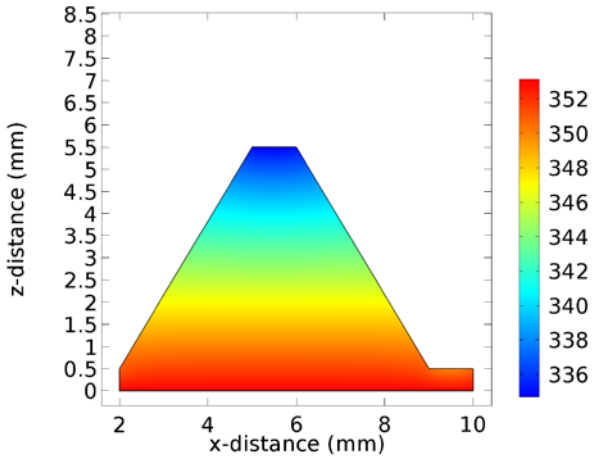

Figure 2 COMSOL simulation of the thermal profile for a 3D-printed object in ABS, with W = 25 mm, L_h = 3 mm, h = 5 mm, when the difference between the hot side and room temperature is set to 60 K.

recently proposed to use an out-of-plane thermal gradient, while retaining the benefits of printed electronics, is the development of printed thermocouples with unneglectable vertical dimension [11]. This result can be achieved depositing thin film thermoelectric materials upon thick 3D printed vertical structures, as presented in Figure 1. With this approach, the insulating thick structure will help retaining a temperature separation between top and bottom side ($\Delta T_H T_C$), and the thermoelectric material will be able to generate a proportional thermovoltage. In this contribution, we systematically investigate the voltage and power, which can be potentially generated by such structures, using as active thin film thermoelectric nanocomposites explored in recent literature. The rest of this paper is structured as follows. In Section II, we briefly describe the methods employed for the thermal and electrical simulations. Subsequently, in Section III we describe the evaluation of an explicit function for the thermal gradient (III.A), followed by a calculation of the theoretical power (III.B) and by the comparison of results for different active materials.

II. METHODS

A. Thermal Simulations

The geometrical structures have been drawn in a commercial multi-physics simulation toolbox (COMSOL Multiphysics®). The material considered for the bulk 3D substrate is Acrylonitrile Butadiene Styrene (ABS), as it is commonly employed in desktop 3D-printers. The simulations were performed sweeping the temperature of a *hot-side* (i.e., the bottom of the structure depicted in Figure 1b), considering conduction and convection heat dissipation on all the surfaces, given an ambient temperature of 293 K.

B. Electrical Power Estimation

The generated power was estimated utilizing the theoretical formula conjunctly with the semi-empirical model

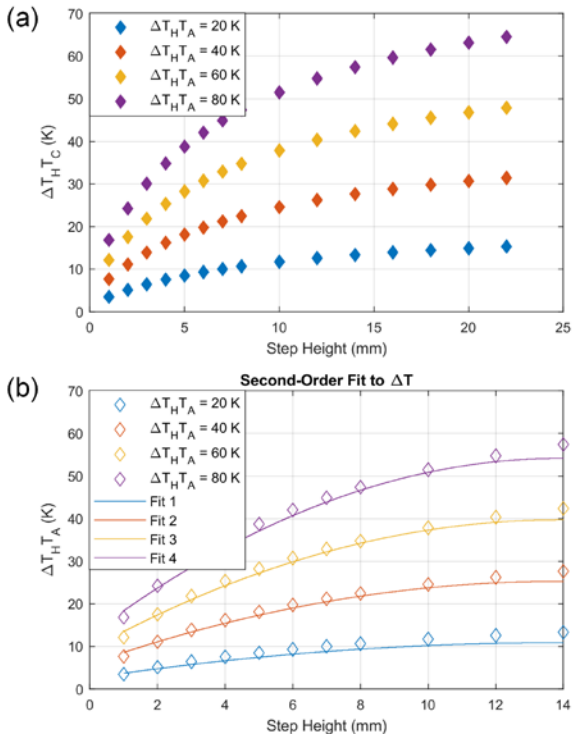

Figure 3. Panel (a) presents the simulated temperature gradient between hot side and cold side of the 3D-printed structures, as a function of the step height h and parametrized with the temperature of the hot side. Panel (b) is a reduced version of the same curves, considering showing that the considered polynomial fit is sufficiently accurate, when the step height is below 12 mm

described in the "Discussion and Results". The electrical and thermoelectrical characteristics of the considered materials were extracted from the works of Suemori et al. [12], Montgomery et al. [13], Lu et al. [14] and our own laboratory measurements.

III. DISCUSSION AND RESULTS

A. Evaluation of the thermal gradient

The multiphysics simulations show how the thermal gradient across the 3D structure is strongly dependent on the difference between room temperature and the hot side $\Delta T_H T_A$, and the step height h. A typical result is presented in Figure 2, with a width of the structure equal to 25 mm and a step height of 5 mm, when $\Delta T_H T_A = 60K$. The gradient retained by the structure is circa 28 K, which is a remarkable value. On the other hand, Figure 3 (a) shows the variation of $\Delta T_H T_C$ as a function of the step height, and parametrized to the gradient $\Delta T_H T_A$. Albeit an exact analytical representation of the phenomena might require a more in-depth analysis, by restricting the domain to small step height (i.e., h < 14 mm), it is possible to effectively approximate the behavior of the gradient with respect to h with a family of second order polynomial curves:

$$\Delta T_H T_C = \Delta T_H T_A * (a_2 h^2 + a_1 h + a_0) \qquad (1)$$

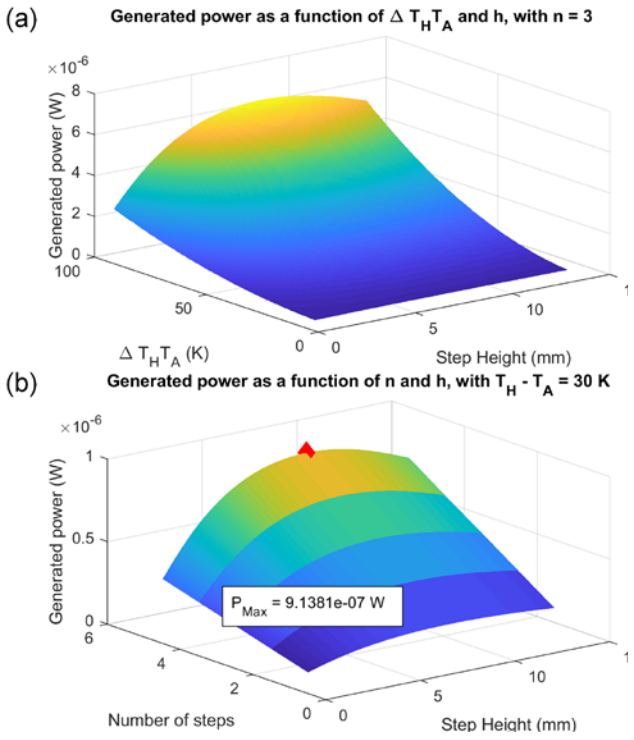

Figure 4. The output of the calculations using the theoretical formula and the semi-empirical model are collected in a series of plots, summarizing the theoretically acheivable power as a function of the step height versus $\Delta T_H T_A$ (a) and the number of steps (b)

with $a_2 = -0.0029, a_1 = 0.0796$ and $a_0 = 0.1680$, yielding an adjusted $R^2 = 0.99$.

B. Calculation of the Generated Power

First, given the electrical, thermoelectric and geometrical characteristics of the system, we calculated an analytical formula to describe the dissipated power in the considered structures. Electrical power will simply be:

$$P = \frac{V^2}{R_T} \quad (2)$$

where R_T is the total resistance of the thin film, and V is the generated thermovoltage between the left and the right side. Defining an effective Seebeck Coefficient α, as the average between the coefficients of the p-type and the n-type material, and n, as the number of periodic cells, it is possible to write:

$$V = n\,\alpha\,\Delta_T(h) \quad (3)$$

Concerning the overall resistance, it can be evaluated as the sheet resistance of the thin film, multiplied by the total length and divided by the width W. The latter is a design parameter, while the former can be evaluated as 2n times the sum of the horizontal connecting steps and the oblique walls. In formulas:

$$L_T = 2n\left(\frac{h}{\sin(\gamma)} + S\right) \quad (4)$$

$$R_T = \frac{R_{sh} L_T}{W_T} \quad (5)$$

Combining (2) – (5), a final expression for the electrical power can be derived as:

$$P = \frac{2\,n\,\alpha^2\,W\sin(\gamma)}{R_{sh}(h + S\sin(\gamma))}\Delta T^2(h) \quad (6)$$

This formula highlights a linear dependency of the power from the number of periodic cells, and a proportionality to the square of the temperature gradient. As shown in the previous section, however, the temperature gradient can be approximated with sufficient accuracy by a second order polynomial curve. By plugging (1) in (6) it is possible to have an approximation of the theoretical generated power as a function of all the geometrical, thermoelectric and electrical parameters. The resulting equation (not shown, as it is just as informative as (6)) can then be used for a simple calculation or for parameters optimization purposes.

C. Comparison of different nanomaterials

In order to find the effectiveness of such structure, a series of different nanomaterials from previous literature was considered. Since, as we previously showed [15], solution-processable nanomaterials can be deposited in-situ on 3D-printed objects, we selected the most promising thermoelectric nanomaterials considered in current literature [11]–[14]. In the first three works, the materials are employed by the respective research groups for the realization of planar devices, while the last work is our preliminary proof-of-concept of 3D-printed out-of-plane thermocouples. In every case, the sheet resistance was calculated as the ratio of the conductivity to a layer thickness of 1 μm. The outputs of our calculation script are shown in Figure 4, which presents the generated power as a function of $\Delta T_H T_A$ and h, with fixed n (a) and power as a function of n and h with given $\Delta T_H T_A$ (b). The curves provide a useful toolbox for the choice of the optimal geometrical parameters. For instance, combining the results, it is possible to estimate the optimal h and the minimum number of periodic cells to achieve a target power, with a constraint on the temperature difference.

Calculations performed on the different nanomaterials yield a complete picture on the efficiency of the different materials, when employed in the proposed out-of-plane configuration. Particularly, as presented in Figure 5 (a), among the Carbon Nanotubes (CNT)-based nanocomposites, the top performer resulted to be the one presented by Suemori et al. [12], because of its elevated conductivity, due to high-purity Single Walled Carbon Nanotubes. The best performances, however, would be obtained employing the aqueous dispersion of $(Sb, Bi)_2(Te, Se)_3$ nanowires, as presented by Lu et al. [14]. Finally, to evaluate the maximum power generated by this material, the simulations were re-iterated for different thickness of the thermo-active layer (1 μm to 5 μm). While still keeping the thickness below a

 ISBN: 978-1-61208-621-7

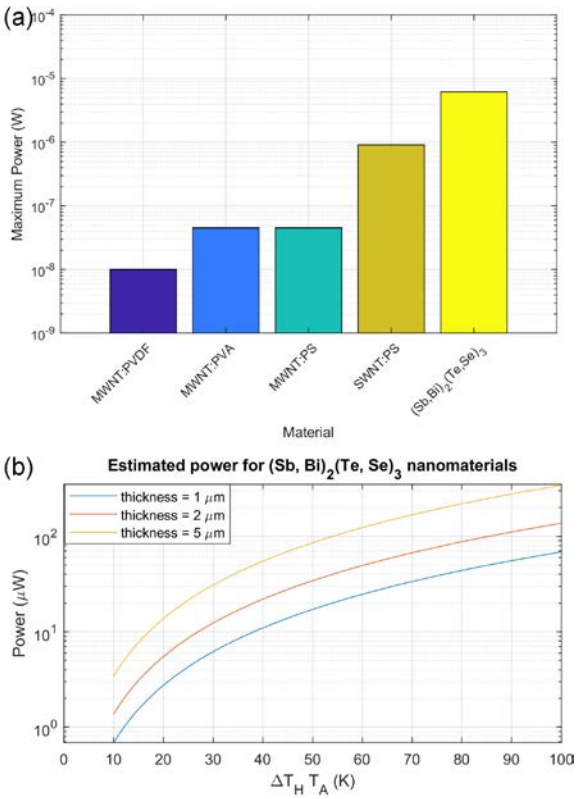

Figure 5. Panel (a) presents the maximum theoretical power for the different materials, estimated for a structure made of 5 periods at a temperature difference between the room and the hot side equal to 30 K. The bottom figure (b) presents an estimate of power for different active layer thickness.

reasonable target for common deposition methods, such as spray-deposition, this approach would yield even superior results: the generated power, with $\Delta T_H T_A = 100\ K$, can easily exceed the hundreds of microwatts.

IV. Conclusion

In this contribution, we introduced further advances towards the obtainment of a fully printed, cost-effective, out-of-plane thermocouple. In our previous work, we presented three different 3D geometries, choosing the one with the best trade-off between the ability to keep the thermal gradient, and the overall produced voltage. Here, we present a comprehensive theoretical calculation of the maximum power that can be generated by such structures, applied to some known nanomaterials. The final results show how most of the CNT-based nanocomposites could generate few microwatts with a very limited temperature gradient. They, however, underperform, when compared to $(Sb, Bi)_2(Te, Se)_3$ nanowires. Although these values are smaller than what previously reported in literature for printed thermocouples, the scenarios in which out-of-plane thermal gradients are required (e.g., body temperature, vehicle engine) are much more likely than for the planar counterparts. Finally, these sensors can be employed either as harvesters to power up sensor modules, or as energy-autonomous temperature sensors.

For this reason, we believe this novel approach will be a significant step forward in the realization of cost-effective, energy-efficient and environmental-friendly sensor nodes for the Internet of Things.

Acknowledgement

The authors acknowledge the support of ASK Industries SpA. The project was partially funded by the Ministry of Economic Development through the “Vehicle Active Sound Management” project.

References

[1] McKinsey & Company, “The Internet of Things: Mapping the Value beyond the Hype,” 2015.

[2] H. Bauer, M. Patel, and J. Veira, “The Internet of Things: Sizing up the opportunity,” *McKinsey&Company - High Tech*, 2014. .

[3] A. Zanella, N. Bui, A. Castellani, L. Vangelista, and M. Zorzi, “Internet of Things for Smart Cities,” vol. 1, no. 1, pp. 22–32, 2014.

[4] J. Roberts, N. Jackson, and M. Smith, *Tree roots in the built environment*. TSO (The Stationery Office), 2006.

[5] W. Honda, S. Harada, T. Arie, S. Akita, and K. Takei, “Wearable, human-interactive, health-monitoring, wireless devices fabricated by macroscale printing techniques,” *Adv. Funct. Mater.*, vol. 24, no. 22, pp. 3299–3304, 2014.

[6] C. Perera and C. H. I. H. Liu, “The Emerging Internet of Things Marketplace From an Industrial Perspective : A Survey,” *IEEE Trans. Emerg. Top. Comput.*, vol. 3, no. 4, pp. 585–598, 2015.

[7] A. Falco, J. F. Salmerón, F. C. Loghin, P. Lugli, and A. Rivadeneyra, “Fully Printed Flexible Single-Chip RFID Tag with Light Detection Capabilities,” *Sensors*, vol. 17, no. 3, p. 534, 2017.

[8] K. Suemori, S. Hoshino, and T. Kamata, “Flexible and lightweight thermoelectric generators composed of carbon nanotube-polystyrene composites printed on film substrate,” *Appl. Phys. Lett.*, vol. 103, no. 15, pp. 153902-1-153902–4, 2013.

[9] Z. Lu *et al.*, “Fabrication of flexible thermoelectric thin film devices by inkjet printing,” *Small*, vol. 10, no. 17, pp. 3551–3554, 2014.

[10] A. Albrecht *et al.*, “Transparent Thermocouples based on Spray-coated Nanocomposites,” in *IEEE Sensors 2017 (in press)*, 2017.

[11] A. Falco, P. Lugli, F. C. Loghin, and A. Rivadeneyra, “Design, Simulation and Fabrication Strategies for Printed Out-of-Plane Thermoelectric Devices,” in *IEEE Sensors 2017 (in press)*, 2017.

[12] K. Suemori, Y. Watanabe, and S. Hoshino, “Carbon nanotube bundles/polystyrene composites as high-performance flexible thermoelectric materials,” *Appl. Phys. Lett.*, vol. 106, no. 11, pp. 113902-1-113902–5, 2015.

[13] D. S. Montgomery, C. A. Hewitt, R. Barbalace, T. Jones, and D. L. Carroll, “Spray doping method to create a low-profile high-density carbon nanotube thermoelectric generator,” *Carbon N. Y.*, vol. 96, pp. 778–781, 2016.

[14] Z. Lu *et al.*, “Aqueous solution synthesis of (Sb, Bi)2(Te, Se)3 nanocrystals with controllable composition and morphology,” *J. Mater. Chem. C*, vol. 1, no. 39, p. 6271, 2013.

[15] A. Falco, M. Petrelli, E. Bezzeccheri, A. Abdelhalim, and P. Lugli, “Towards 3D-Printed Organic Electronics: Planarization and Spray-Deposition of functional layers onto 3D-printed objects,” *Org. Electron.*, vol. 39, pp. 340–347, 2016.

 ISBN: 978-1-61208-621-7